Saidj, Faiza and Kibboua, Rachid and Azzi, Abdelwahid and Ababou, Noureddine and Azzopardi, Barry J. (2014) Experimental investigation of air–water two-phase flow through vertical 90° bend. Experimental Thermal and Fluid Science, 57 . pp. 226-234. ISSN 0894-1777

Experimental investigation of air-water two-phase flow through vertical 90° bend

Faiza Saidj[1], Rachid Kibboua[1], Abdelwahid Azzi[1], Noureddine Ababou[2], Barry James Azzopardi[3]

1 Université des Sciences et de la Technologie Houari Boumedien, LTPMP/FGMGP, BP 32 El Alia, Algiers 16111, Algeria

2 Université des Sciences et de la Technologie Houari Boumedien, LINS/FEI, BP 32 El Alia, Algiers 16111, Algeria

3 Process and Environmental Research Division, Faculty of Engineering, University of Nottingham, University Park, Nottingham NG7 2RD, UK

Corresponding author E-mail address: faiza78saidj@yahoo.fr

Abstract

The behaviour of two-phase air-water mixture flowing from the horizontal to the vertical through a 90° bend has been investigated experimentally. Cross sectional void fraction at nine positions, three upstream and six downstream of the bend have been measured using a conductance probe technique. The bend, manufactured from transparent acrylic resin has a diameter of 34 mm and a curvature (R/D) equal to 5. The superficial velocity of the air was varied between 0.3 and 4 m/s and that for the water between 0.21 and 0.91 m/s. The characteristics signatures of Probability Density Function (PDF), the Power Spectral Density (PSD) of the time series of cross sectionally average void fraction and visual observations have been used to characterise the flow behaviour. For the experimental conditions, plug, slug and stratified wavy flow pattern occurred in the horizontal pipe while slug and churn flow patterns were present in the vertical pipe. The void fraction increased with the gas superficial velocity. The correlation of Nicklin et al. predicted the structure velocity for the slug flow in both horizontal and vertical pipes reasonably accurately. With regards to the frequency of the periodic structures present, some conditions showed little change from upstream to downstream the bend whilst others showed an increasing in the structure frequency from horizontal to vertical pipe. The slug length increased by passing through the vertical bend.

Keywords : 90° Bend, two-phase flow, void fraction, air-water, conductance probe, flow pattern

1. Introduction

Bends are present in much industrial equipment, e.g., heat exchangers, chemical plants, transport piping, thermal-hydraulic reactor system etc. One peculiar and complex characteristics of the bend flow is the establishing secondary flow, which is already well known from single-phase liquid flow. When the fluid flows through the bend, the curvature causes a centrifugal force, directed from the centre of curvature to the outer wall. This force and the presence of a boundary layer at the wall, respectively fluid adhesion to the wall, combine to produce the secondary flow ideally organised in two identical eddies. Basically, the fluid in the core moves outwards and in the region near the wall inwards. The secondary flow is superimposed to the main stream along to the tube axis, imposing a helical shape to the stream lines Azzi et al. [1].

When positioned vertically, bends involve the simultaneous action of centrifugal, gravitational and buoyancy forces, which leads to complicated flow behaviour such as inhomogeneous phase distribution, flow reversal, flooding, secondary flow and coalescence. These latter can produce corrosion and consequently pipe damage. As consequence, the understanding of the flow behaviour upstream, through and downstream the bend is of prime importance in the design of the devices where they are present.

In single-phase flow several studies are reported in the literature regarding these aspects while in two-phase gas-liquid comparatively less work has be devoted to and more particularly for the vertical 90° bends where very few studies are cited.

Azzopardi [2] in his review on two-phase flow through fittings discussed the flow structure of a two-phase mixture flowing through 90° and 180° bends. He found that there were more publications about 180° bends than 90° ones. Of the papers on the latter type of bends, several were about the pressure losses occurring at the bend such as Azzi et al. [1].

For analysing the two-phase mixture flowing in a circuit including a 90° bend three flow orientations have been investigated. Vertical to horizontal Gardner and Neller [3], Maddock et al. [4] and Abdulkadir et al. [5]; horizontal to horizontal Ribeiro et al. [6], Sekoguchi et al. [7], Sánchez Silva al. [8]; horizontal to vertical .Legius [9], Omebere-Iyari and Azzopardi [10].

Table 1.summarizes the orientation and the pattern of the flow by author.

Table 1. Two-phase flow orientation

Author	**Upstream pipe**	**Downstream pipe**	**Flow upstream**
Gardner and Neller [3]	Vertical	Horizontal	Annular
Maddock et al. [4]	Vertical	Horizontal	Annular
Abdulkadir et al. [5]	Vertical	Horizontal	Bubbly, Slug, Churn
Ribeiro et al. [6]	Horizontal	Horizontal	Annular
Sekoguchi et al.[7]	Horizontal	Horizontal	Slug
Sánchez Silva et al. [8]	Horizontal	Horizontal	Slug
Legius [9]	Horzontal	Vertical	Slug
Omebere-Iyari and Azzopardi [10]	Horizontal	Vertical	Slug

Gardner and Neller [3] reported that for the case of a bubble/slug flow upstream of a 90° vertical bend, in the bend the gas can flow either on the outside or the inside of the bend depending on the balance between the centrifugal force tending to push the liquid phase to the outside and the gravity forcing it to the bottom, resp, inside. The competition between these two forces is expressed by a Froude number, $Fr_\theta=V^2/gR\sin\theta$, where V is the mixture mean velocity, R the radius of curvature of the bend and θ the bend angle. It is claimed that both phases are flowing in radial equilibrium when the Froude number is equal to unity : for a value in excess of one the gas is displaced to the inside of the bend, while in the other case of a number less than unity the gas moves to the outside of the bend.

In order to study the repartition of the film thickness of an annular flow through 90° bend, Maddock et al. [4] used a series of 30 to 90° bends at the top of a vertical pipe. They reported the results of the circumferential variation of the film thickness as well as the cross sectional variation of the droplet flowrate.

More powerful modern advanced instrumentation, Electrical Capacitance Tomography (ECT) and the Wire Mesh Sensor (WMS), was employed by Abdulkadir et al. [5] to analyse the effects of a 90° bends on two-phase gas-liquid flow. The ECT probes were mounted 10

diameters upstream of the bend whilst the WMS was positioned either immediately upstream or immediately downstream of the bend. The downstream pipe was kept horizontally while the upstream one was positioned either vertically or horizontally. The characteristics signatures of Probability Density Function (PDF) obtained from the time series of cross-sectionally averaged void fraction data were utilized to identify the flow pattern upstream and downstream the bend. They remarked that bubble, stratified, slug and semi-annular flows were present downstream the bend for the vertical 90° bend while for the horizontal 90° bend, the flow pattern exhibited the same configurations as upstream the bend.

By using the Laser diffraction technique, Ribeiro et al. [6] measured the Sauter mean diameter of the drops upstream and downstream a horizontal 90° bend. They found that the bend increases the diameter of the drops. They suggested that this increasing is the result of several processes occurring at the bend, such as drop coalescence and deposition and re-entrainment.

The static pressure along pipes upstream and downstream 90° bends,with both pipes on a horizontal plane, was measured by Sekoguchi et al. [7] using water manometers. They found that the maximum value of the recovery length downstream the bends was about 150 pipe diameters for the flow conditions and bend geometries investigated, while the upstream developing length was found considerably smaller.

Using conductive probes consisting of pairs of flush mounted metal rings, Sánchez Silva et al. [8] measured the slug hold-up, length and frequency of slug upstream and downstream of a horizontal 90° bend. Upstream of the bend measurement devices were positioned at a distance from mixer where fully developed slugs where found, while downstream the bend, the measuring station was placed near the bend where the flow is not fully developed. They noticed that the slug flow characteristics (velocity, frequency, hold-up, length) downstream the bend are greatly different to those upstream the bend in the fully developed slug flow region.

Legius [9] analyzed the effects of a vertical 90º bend on the two-phase flow behaviour in a flow line/riser system experimentally and numerically. He found that slug formation is promoted by the presence of the bend. Under most of the experimental conditions studied, a fully developed slug was observed just downstream the bend. At higher flow rates is can develop into churn flow. The slug in the riser part is the origin of a continuous process of liquid fall-back to the upstream horizontal duct through a liquid film. This liquid film is moved upstream as waves, destabilizing the horizontal stratified flow in the process.

Moreover, by using a visualization technique and responses of the pressure transducers, the author proposed flow regime maps for the horizontal pipe and the riser respectively. However no details concerning the slug characteristics (structure velocity, length and frequency of the slug) are given.

Omebere-Iyari and Azzopardi [10], presented the time varying void fraction data and flow pattern information for the two-phase nitrogen-naphtha mixture flowing in a 189 mm diameter and 52 m high and compared their results for the same riser when it was connected to an upstream horizontal pipeline of the same diameter. They found that the slug flow formed in the upstream horizontal pipeline at high liquid flowrates is propagated into the vertical pipe and is absent in the same riser when the gas and liquid phase are introduced at the riser base.

It appears from this review that there is a lack in the analysis of the behaviour of gas-liquid mixture passing through a circuit constituted by a flow line, a 90° bend and a riser; and more particularly downstream the bend. The present work is an attempt to fill this gap.

2. Experiments

A schematic diagram of the experimental apparatus installed at the Laboratory of Multiphase Flows and Porous Media of the University of Sciences and Technology Houari Boumedien, Algiers, is shown in Figure 1.

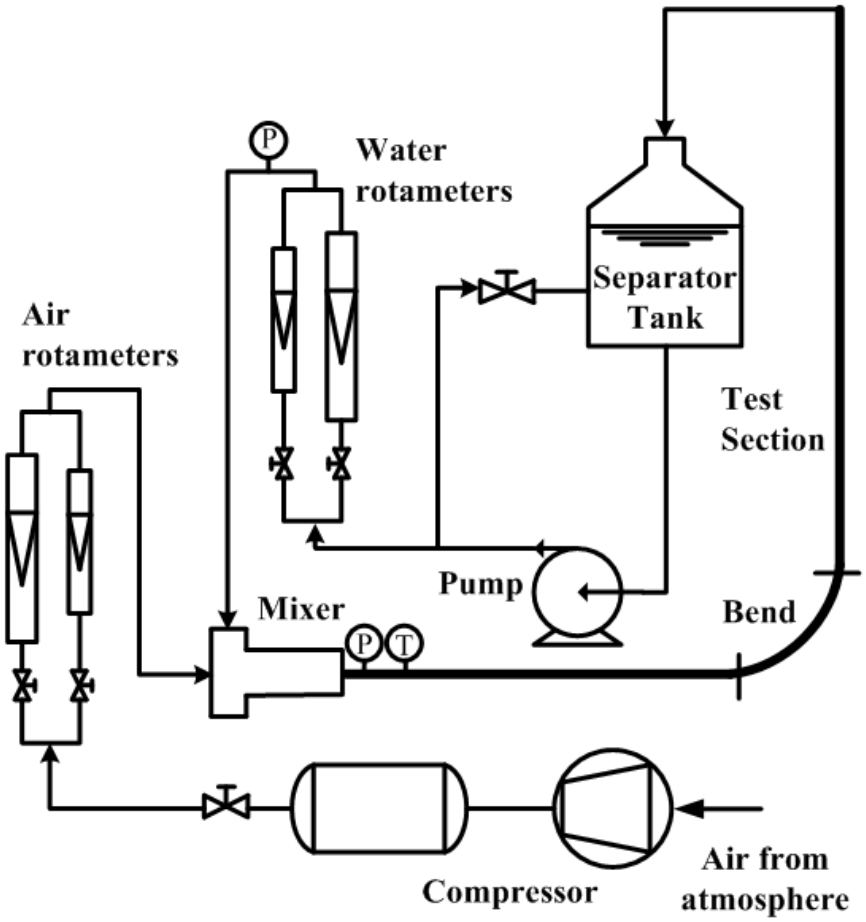

Fig. 1 Schematic diagram of the experimental facility

The test section consists of a horizontal pipe preceding a 90° the bend and followed by a vertical outlet pipe. Each pipe was 5m long (about 150 pipe diameters to ensure the full development of the flow). These pipes are made from transparent acrylic resin (PMMA), which permitted observation of the flow pattern. The inner diameter and the thickness of the straight pipes are 34 mm and 4 mm respectively. The 90° bend made in Perspex has been machined using a CNC machine. Thus, after achieving geometrical pieces in the shape of half torrus with 17 mm from plates of 20 mm thickness, these pieces are glued, bolted and pasted to the flanges to give the final form of the bend. The relative bend curvature is equal to 5.

The mixing unit (Mixer) made of Polyvinyl chloride (PVC), is consisted of a section of pipe wall with 64 holes with 1 mm diameter spaced equally in 8 columns over a length of 80 mm. The liquid was introduced into an annular chamber surrounding this section of pipe, creating thus, a more even circumferential mixing effect.

The water is drawn by pump from a storage tank acting as two-phase separator to the mixer where it is mixed with air supplied from the compressor. This latter is an electro-compressor (GIS, GS/35/500/600) of 500 l capacity, 11 bar maximum pressure and 600 l/min maximum flowrate.

Downstream the mixer, the air-water mixture flows through the flow line (horizontal pipe), the bend, the riser (vertical pipe) and finally to the storage tank, where the gas and liquid phase are separated. The water is recirculated and the air is released to the atmosphere.

Air and water flowrates are measured using one each of the rotameters (variable area meter with rotating float) mounted in parallel before the mixing unit. Two for the gas phase (1 -15 l/min) and (15 – 150 l/min); and two for the liquid phase (50 – 400 l/h) and (0.5 m^3 – 3 m^3/h). The maximum uncertainties in the liquid and gas flow rate measurements are 2%. The static pressure of air is measured prior entering the mixing section. A thermometer with a precision of 0.1°C is used for temperature measurement.

The conductance probe technique has been chosen to measure the average void fraction in the cross section of the pipe. The void fraction is by definition the section occupied by the gas phase divided by the cross section of the pipe. Water behaves as an electrical conducting solution and air as resistive medium. In this technique, the cross-sectional averaged void fraction can be estimated once the relationship between electrical impedance and phase distribution has been established. Tsochatzidis et al. [11], Fossa [12], Abdulkadir et al. [13] are among other researchers who used this technique successfully.

Nine ring-shaped plate conductance probes were installed (Fig.2). Three upstream the bend, at 1175, 660 and 145 mm and six downstream the bend at 145, 660, 1175, 1690, 2205 and 2720 mm respectively from the bend. The first probe is installed at 3935 mm distance after the mixer.

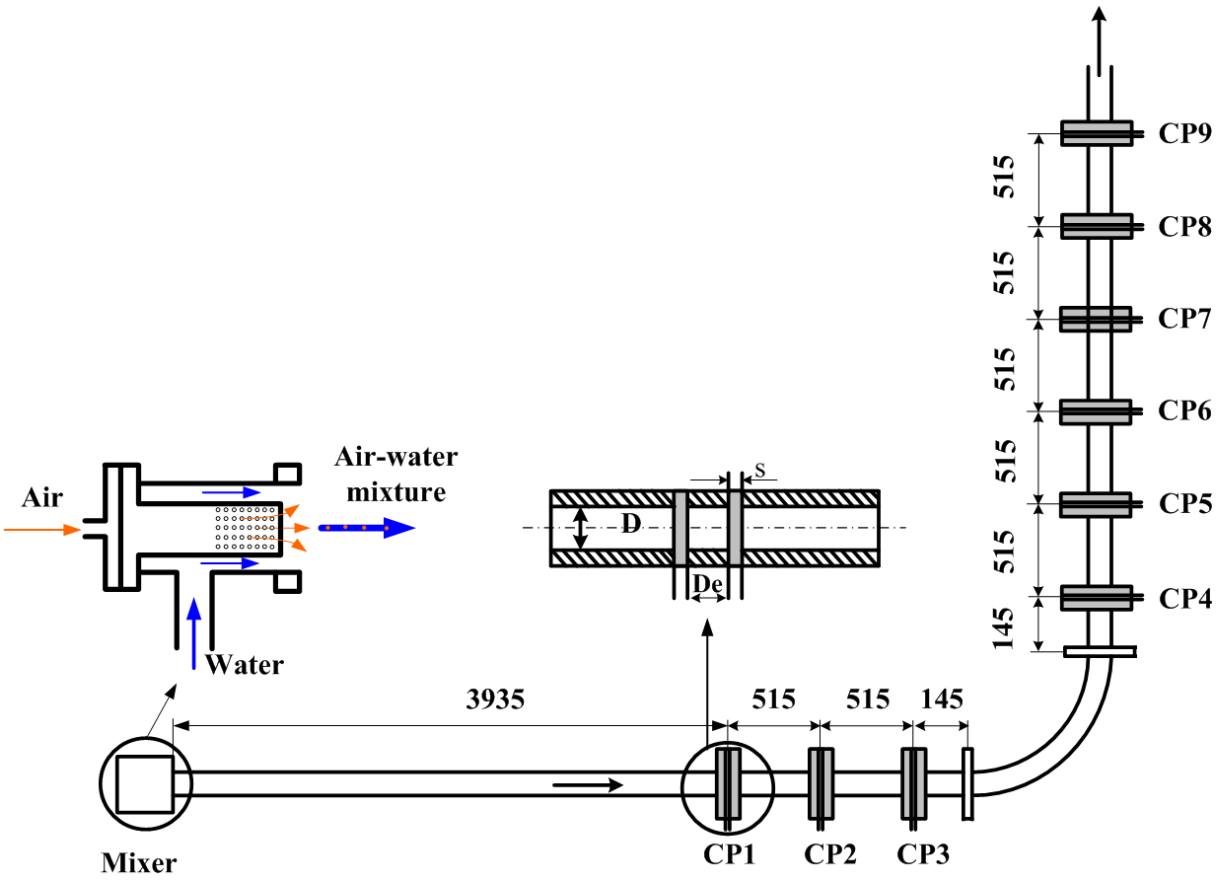

Fig.2 Repartition of the conductance probes along the test section

The probes were constructed by mounting two stainless steel plates between a set of acrylic blocks and machining a hole through them so that they were flush with pipe inner wall. The configuration is characterised by the thickness of electrodes, s, and the distance between them, D_e.The dimensions D_e/D_t and s/D_t were 0.264 and 0.058 respectively.

For measurement purpose an in-house conditioning electronic circuit has been developed. 1V-100kHz excitation voltage has been applied to this circuit. After dc component elimination, amplification, rectification and filtering the signals are sent to data acquisition unit. This latter is constituted principally of PC and Data acquisition Card (16 bits NI DAQ card-6062E) and LabView 8.6 software from National Instrument. Data were taken at a sampling frequency of 200 Hz over 30 seconds for each run. A diagram of the electrical conditioning circuit is given in figure 3 and detailed description of the proposed electronic circuit is presented in Morsi [14] and Morsi et al. [15].

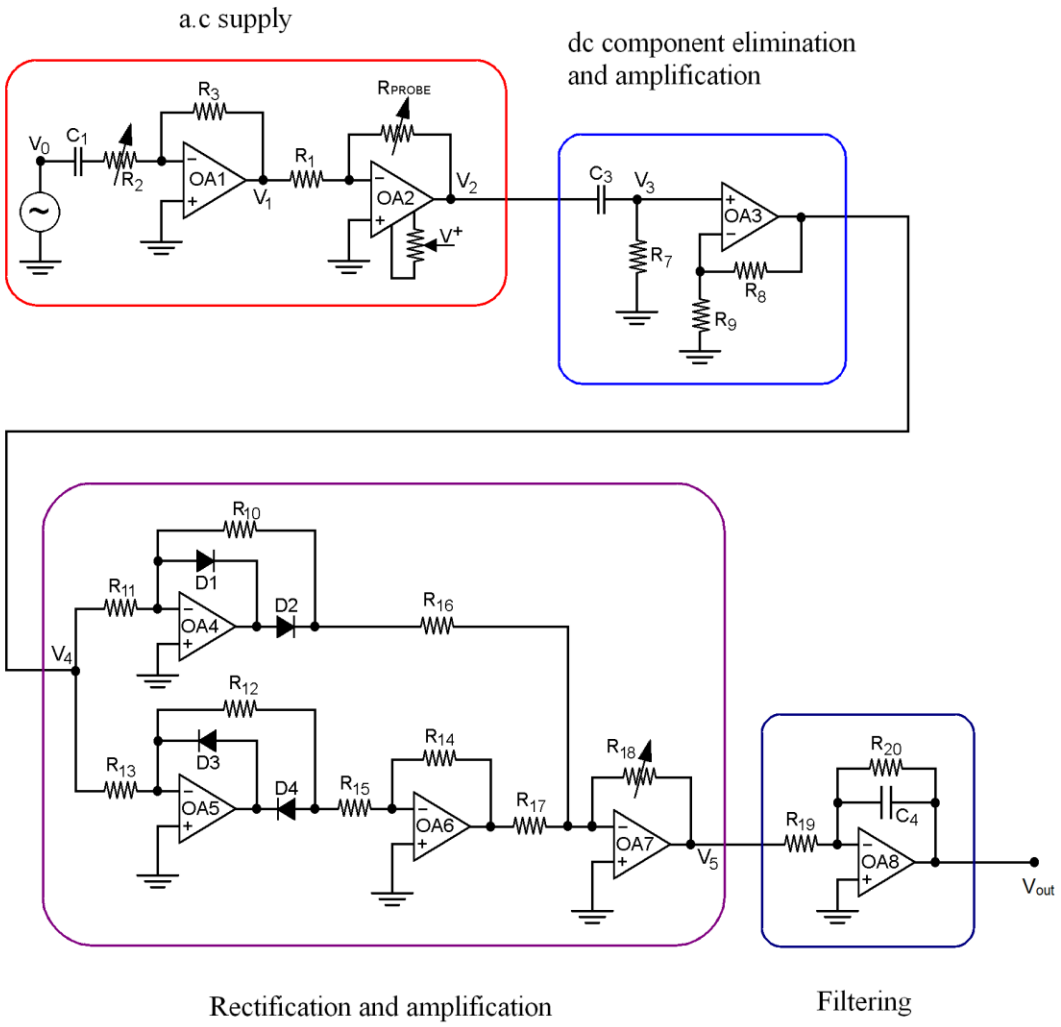

Fig.3 Schematic diagram of the electrical conditioning circuit Morsi et al. [15]

In the present study, the probes have been excited by signal of 100 kHz frequency, in such a way that the imaginary part of the impedance becomes negligible with respect to the real part. The impedance is therefore purely resistive.

The output voltage (V_{out}) given by the probe is proportional to the resistances of the two-phase mixture. This response is converted to dimensionless conductance (Ge^*) by referring to the value obtainable when the pipe is full of liquid (V_{full}). To account for the variation in water resistance, V_{full} was measured before every experimental run and adjusted if a considerable deviation was observed. The calibration procedure consisted in artificially creating instantaneous liquid fractions over the conductance probes. Thus, the insertion of plastic cylinder (of diameters between 10.22 and 33.24 mm), strings of beads (3.99 and 7.66 mm diameter) as well as introducing a known liquid volume into the cylindrical horizontal

pipe were used for simulating the annular, bubbly and stratified flows respectively. Further details on the calibration procedure are also presented in Morsi [14].

3. Results and discussion

3.1 Flow patterns

A series of visual observations made through the transparent walls of the flow line, bend and riser, were carried out for the range of the gas and liquid superficial velocities studied here. Stratified plug, wavy and slug flows were observed in the flow line while slug and churn flows were observed in the riser. To confirm these observations, flow patterns were identified using the characteristic signatures of the Probability Density Function (PDF) of the time series of cross sectionally average void fraction as suggested by Costigan and Whalley [16] and Jones and Zuber [17]. In Figs.4 and 5, the experimental data have been plotted on flow pattern maps of Shoham [18] for the flow line and the riser respectively. Additionally to the present data, those obtained by Legius and van den Akker [19] obtained from similar experiments except the geometrical parameters of the pipes and bend, are plotted on these maps. For the flow line, from Figure 4 one can see that all the experiments of the present study are plug, slug and stratified wavy flows. It can be noticed that the Shoham map predicts the experimental data for the plug and slug flow quite well but is less accurate for the stratified/wavy flow transition. The stratified wavy flow observed in the intermittent region of the map could be attributed to the liquid fall-back from the riser which tends to increase wave generation. On the other hand Shoham map predicts accurately the slug data of Legius and van den Akker but is less good for the stratified flow and the flow they called enhanced slug. In the riser, the present data and those of Legius and Van Den Akker are plotted together in the flow pattern map of Shoham (Fig 5). From this figure it appears that for the present test conditions, the flow patterns observed in the riser are slug and churn flow. The transition between these latter is not so accurately predicted by Shoham. flow pattern map. The same applies to the data of Legius and van den Akker.

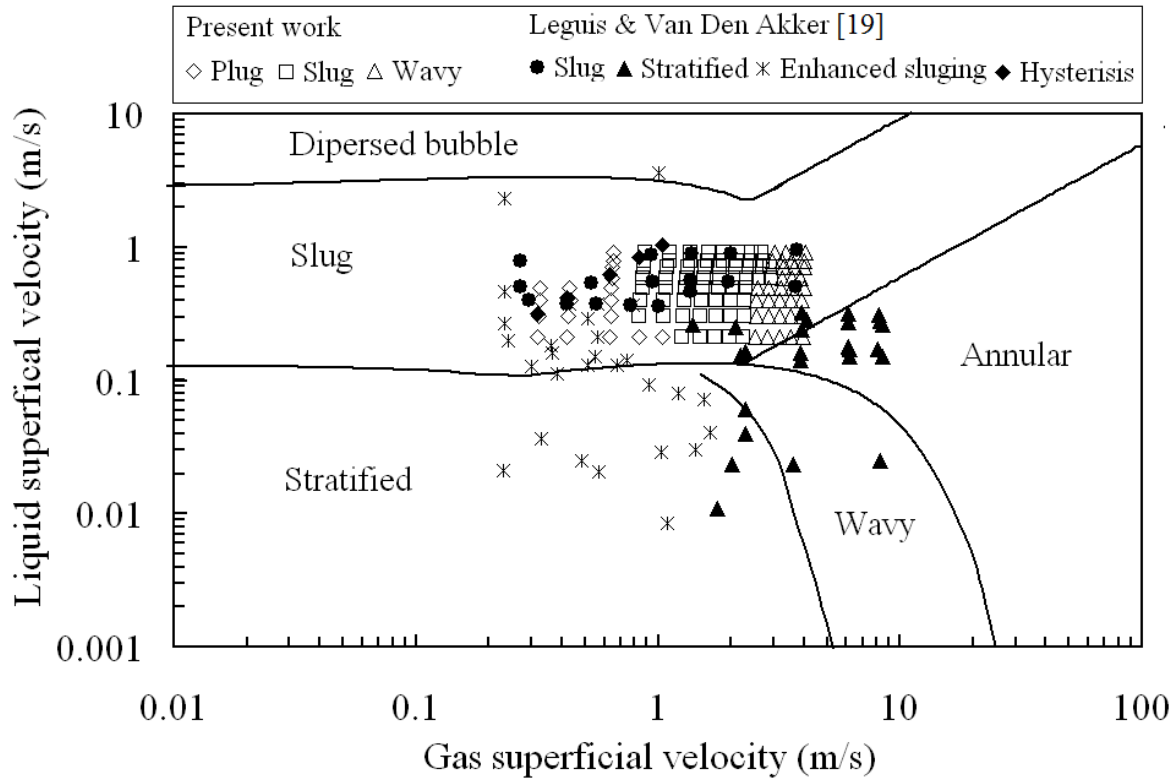

Fig. 4 Flow pattern map in the flow line upstream the 90°bend

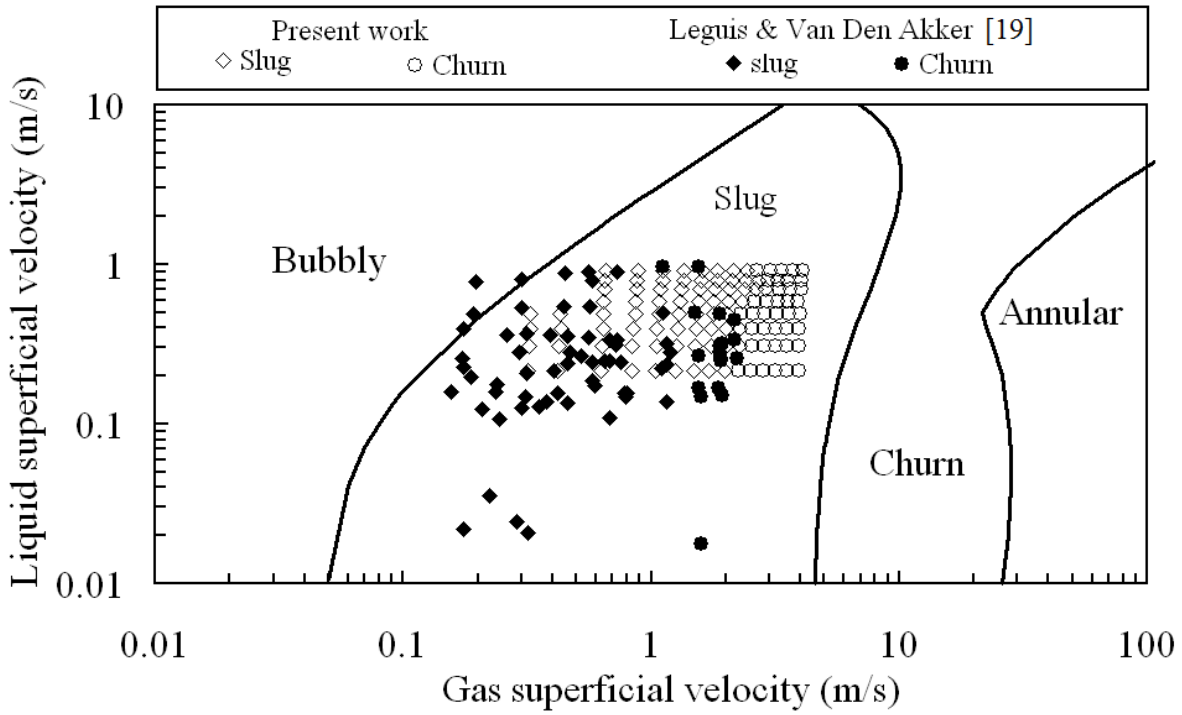

Fig. 5 Flow pattern map in the riser downstream of the 90° bend

3.2. Average void fraction time series upstream and downstream the 90° bend

A sample of the average void fraction time series obtained from the nine conductance probes upstream and downstream the bend (CP1 to CP9) is plotted in figure 6. The superficial velocities are 1.61 and 0.91 m/s for the gas and the liquid respectively. It appears clearly that the bend affects the flow behaviour which can be seen in the time traces of the first conductance probe just after the bend. The flow then, tends to re-establish itself from practically the probe (CP7) where the time series remain the same. This time series shows also clearly the slug flow both upstream and downstream the bend. The void fractions are in proportion to their axial positions. Individual slugs can be clearly traced.

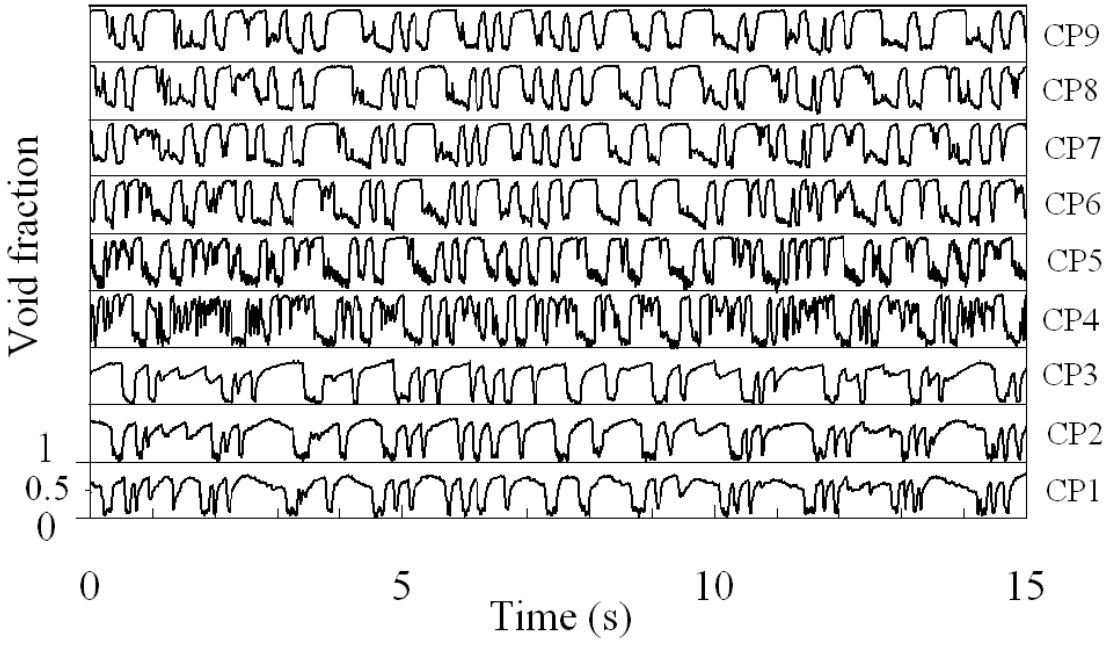

Fig. 6 Average void fraction time series along the test section upstream and downstream the 90° bend, U_{LS}= 0.91, U_{GS}=1.61 m/s

3.3 PDFs of void fraction upstream and downstream the 90° bend

PDF represents the rate of change of the probability that void fraction values lie within a certain range versus void fraction. The total area under the probability density function must equal unity. An example of the evolution of PDFs of the void fraction time series and their dependence on the gas superficial velocity at the superficial liquid velocity equal to 0.49 m/s are represented in Fig.7. Fig. 7(a) represents the PDFs of the average void fraction time series upstream the bend and Fig. 7(b) downstream the bend, the continue line just downstream the

bend and the dashed one the last probe after the bend. For a gas superficial velocity of 0.63 m/s, when the mixture flows through the horizontal line, the PDF shows two peaks; one at a void fraction of 0.56 and a larger one with fluctuations at around 0.09. This is a characteristic of a plug flow having a large gas bubble separated by a liquid containing some small bubbles. After passing through the bend, the larger bubbles coalesce forming Taylor bubbles, leading to the formation of the slug flow. The PDF shows two peaks at void fraction values of 0.1 and 0.92 just after the bend and 0.3 and 0.93 at the topmost probe. This signature is relative to the slug flow with aerated liquid at different Taylor bubble. The difference in the void fraction expresses the difference in gas bubble sizes just after the bend and well downstream of it.

(a)

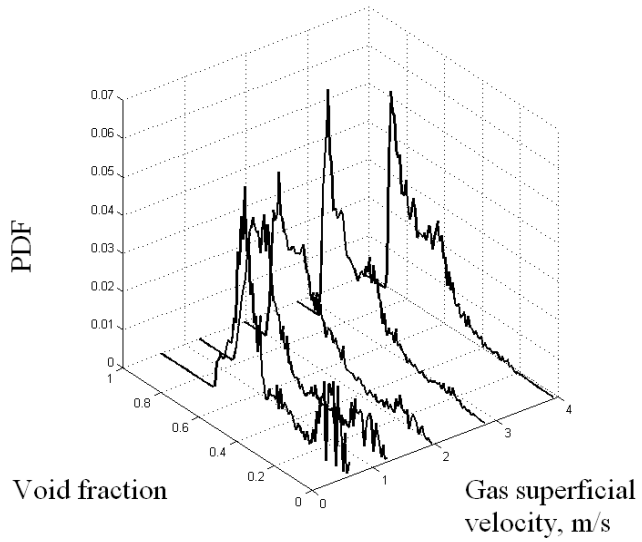

(b)

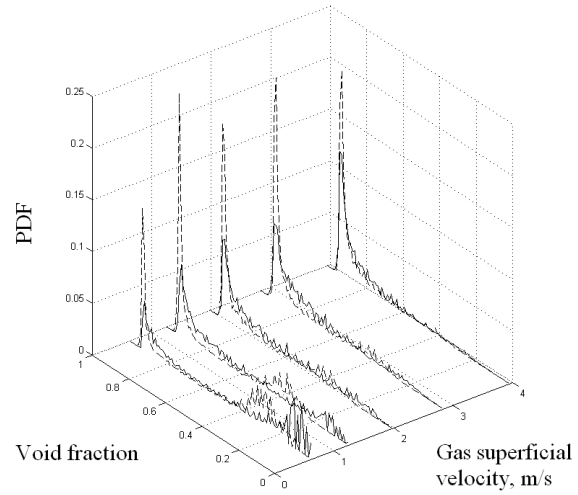

Fig. 7 PDFs of the void fraction function of the gas superficial velocity (a) upstream the bend (b) downstream the bend; continue curve at the first probe downstream the bend, dashed curve last probe downstream the bend; (liquid superficial velocity of 0.49 m/s).

At the highest gas superficial velocity of 3.95 m/s, stratified wavy flow is present in the horizontal pipe. It is characterized by small fluctuations and a high peak with a large base. This increase in the superficial gas velocity intensifies the instability of the liquid slug and

creates the breakup of the Taylor bubbles in the vertical pipe; the churn flow is than observed with a peak at high void fraction with tails extending down to 0.2.

3.4 Cross sectionally average void fraction

The evolutions of the average void fractions upstream and downstream of the bend as function of the gas superficial velocities for a given liquid superficial velocities are plotted in Fig. 8. The filled symbols, (a), correspond to the development downstream the bend and the empty symbols (b) are those upstream the bend. It appears from this figure that for the both pipes the void fraction increases with the superficial velocity. This increasing is more sharply for the low gas superficial velocities than that for high superficial velocities. It can be seen that the void fractions downstream the bend are higher than those upstream the bend. This difference could be explained by the change in the orientation of the flow from horizontal to vertical and the additional effect of centrifugal force created by the curvature of the bend.

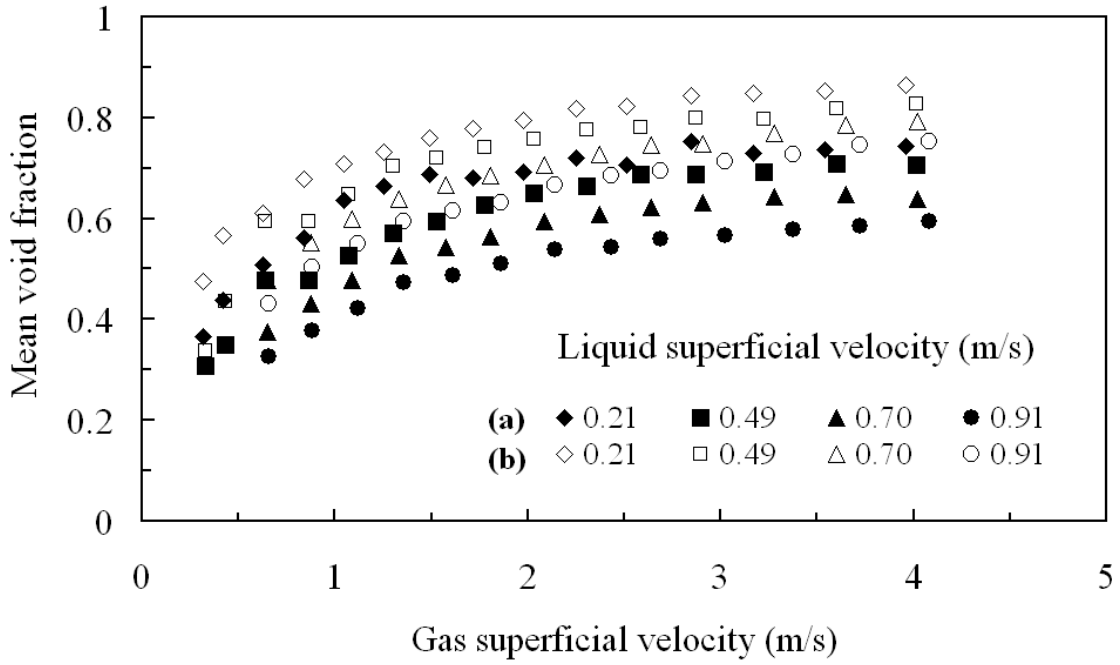

Fig. 8 Average void fractions versus gas superficial velocity (a) upstream and (b) downstream the bend

3.5 Structure velocity

The structural velocity values upstream the bend had been obtained by applying cross correlation analysis to the time series void fraction signals obtained from conductance probes

2 and 3, while the downstream structural velocity was obtained from conductance probes 8 and 9. The structural velocities obtained, as a function of the mixture velocities (U_{GS}+U_{LS}), are exhibited in Fig. 9. Additionally the structural velocity calculated with the equation of Nicklin et al. [20] which is given as Equation (1):

$$U_S = C_0(U_{GS} + U_{LS}) + 0.35\sqrt{gD} \quad (1)$$

Where U_{LS} and U_{GS} are the superficial velocity of the liquid and the gas respectively, D the diameter of the tube, g the acceleration due to gravity and C_0 a coefficient close to 1.2.

In the present study C_0 is found to be equal to 1.12 and the second term of the right side of equation (1) equal to zero as stated by Nicklin et al. that slugs have no tendency to rise in horizontal pipes. The closed symbols relate to the upstream pipe while open symbols correspond to the downstream pipe. It appears from this figure that the structure velocities for the vertical pipe are higher than that of the horizontal one. For low mixture velocities the structure velocities are close to the values predicted by Nicklin et al. equation for both cases, horizontal and vertical tubes; confirming thus the slug pattern of the flow. An increase of the mixture velocity results in a deviation of the points from the predictions of Nicklin et al. curve showing thus the change of the flow from slug to others flow regimes

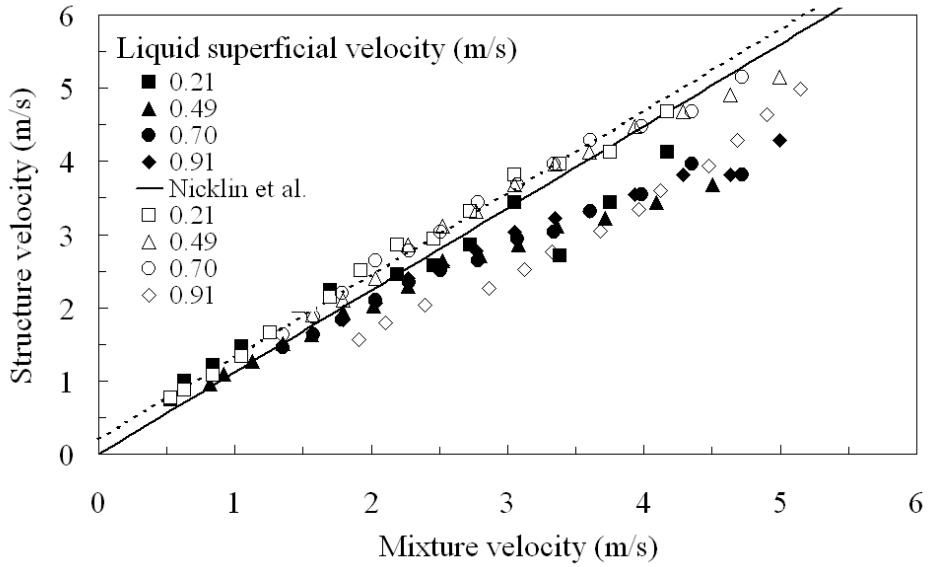

Fig. 9 Structural velocities against mixture velocity upstream and downstream the bend

3.5 Structure frequency

Structure frequency was determined from Power Spectral Density analysis of the time series of cross-sectionally averaged void fraction. It corresponds to the Fast Fourier Transform to the autocorrelation of the time series.

Examples of the variation of the structure frequency along the test section for the low and the high liquid superficial velocities by varying the gas superficial velocity are presented respectively in Figs. 10 and 11.

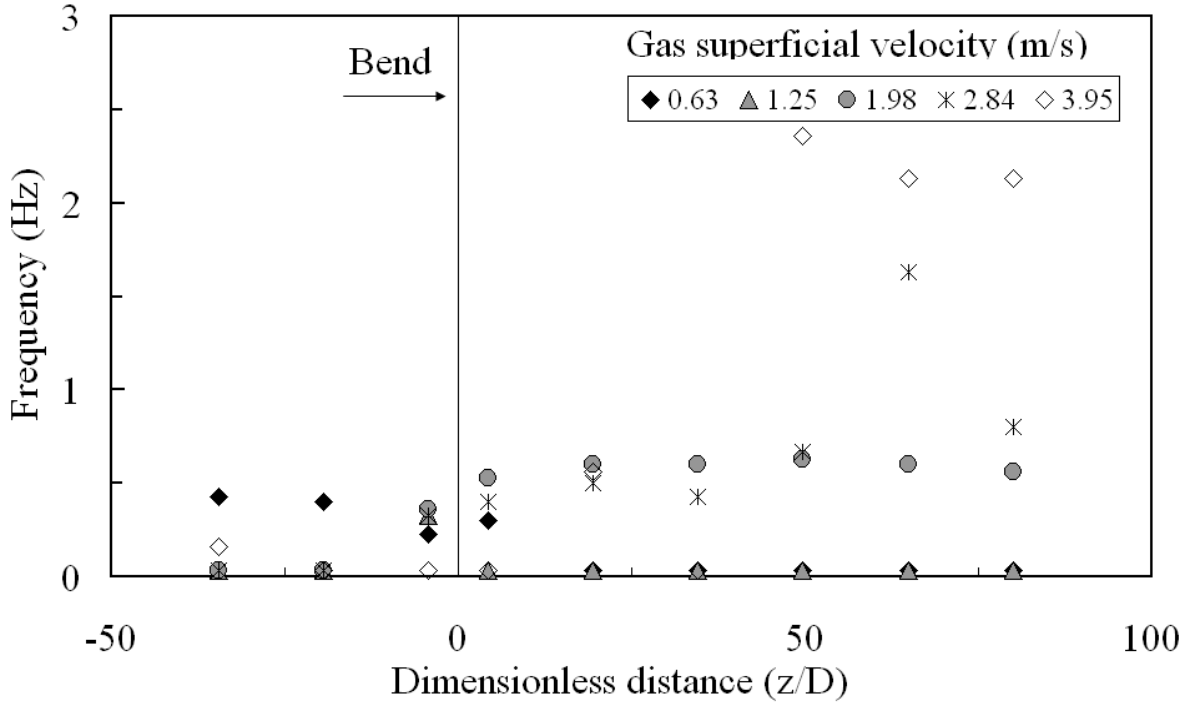

Fig. 10 Evolution of the frequency along the test section for low liquid superficial velocity (= 0.21 m/s)

One can remark that for the case of low liquid superficial velocity the frequency is persistent from horizontal to vertical pipe only for the two lowest gas superficial velocities and increases for the other gas superficial velocities. On the other hand for high liquid superficial velocity, Fig. 11, it is evident that for the all superficial gas velocities the frequency remains persistent.

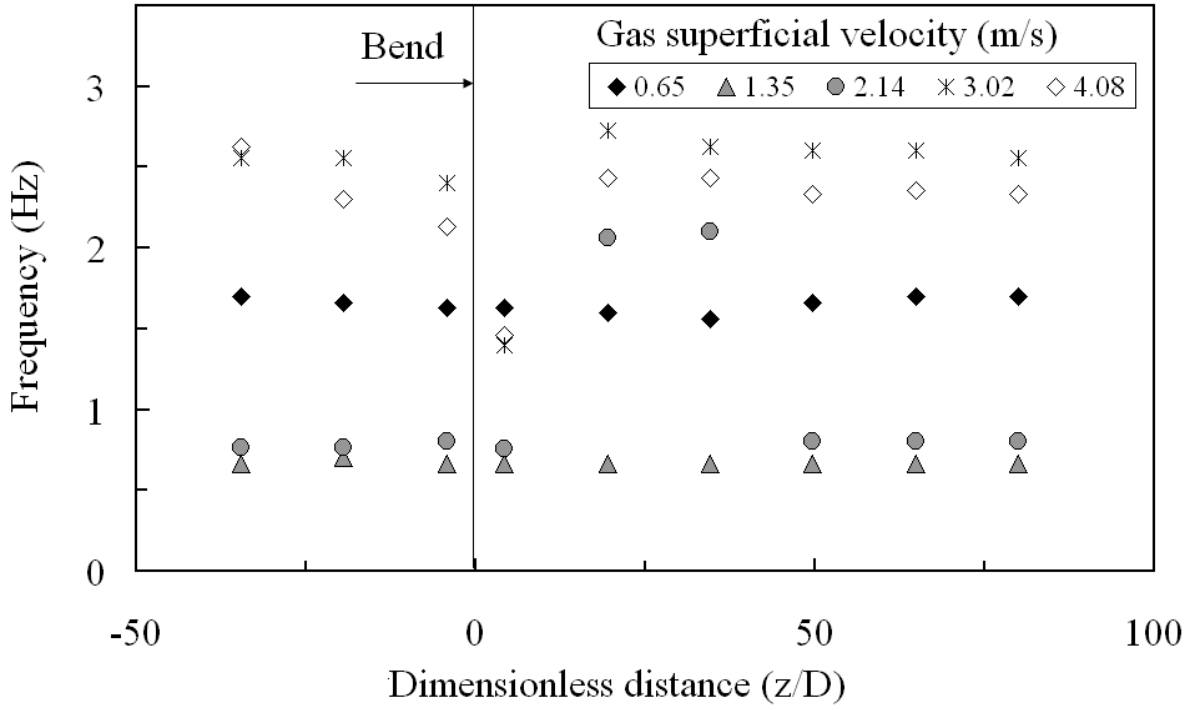

Fig. 11 Evolution of the frequency along the test section for high liquid superficial velocity (Uls=0.91 m/s)

Experimental data are plotted on Shoham flow pattern map respectively for the horizontal (Fig. 12) and the vertical (Fig.13) data. Both figures show the data for either persistency or increasing of the frequency from horizontal pipe to the vertical one.

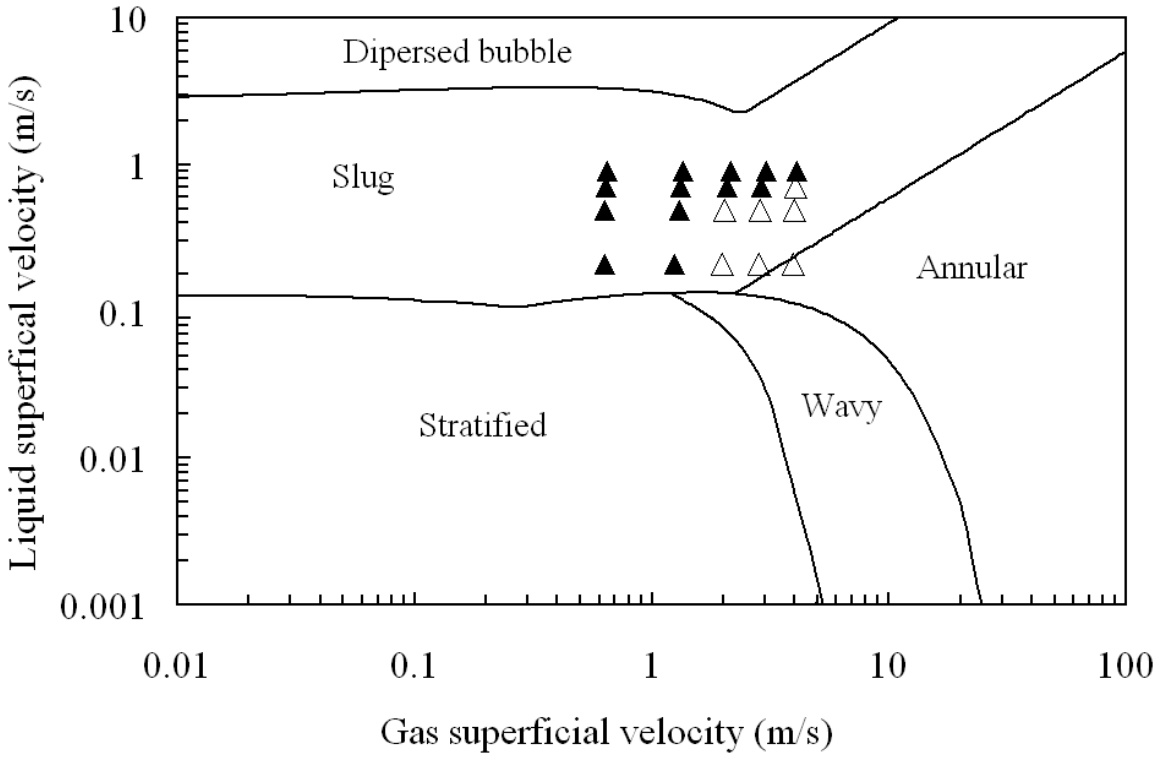

Fig. 12 Plots of the gas and liquid superficial velocities on the Shoham flow map for the horizontal pipe showing the frequency persistence character. Empty symbol correspond to increase in frequency, filled symbols correspond to persistence of frequency

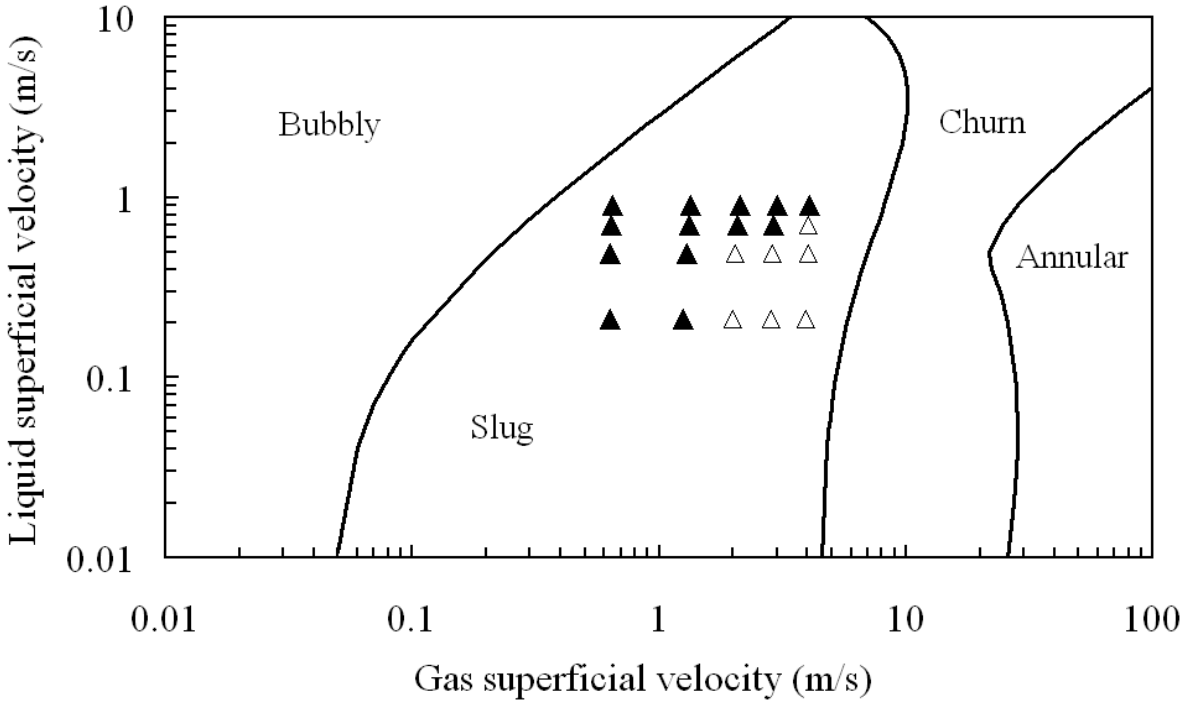

Fig. 13 Plots of the gas and liquid superficial velocities on the Shoham flow map for the vertical pipe showing the frequency persistence character. Empty symbol correspond to increase in frequency, filled symbols correspond to persistence of frequency

The fact that frequency of the periodic structures, particularly in slug flow vary with the angle of inclination of the pipe is illustrated in Fig. 14. This data was obtained using the Wire Mesh Sensor tomographic technique by Abdulkareem [21] using air/silicone oil in a 67 mm diameter pipe which could be set at the angles indicated. It shows how the frequency is much higher for vertical pipes than a horizontal one. This is in contrast to the present work. However, the present system is showing persistence of frequency.

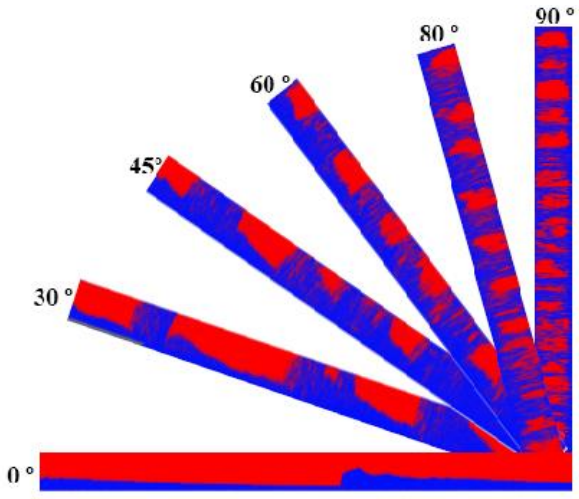

Fig. 14 Effect of inclination on frequency of slugs. Images are time sequences of void distribution across a diameter from Wire Mesh Sensor (WMS) at liquid and gas superficial velocities 0.05 and 0.62 m/s respectively. Abdulkareem [21]

The frequencies of the periodic structures obtained in the present work have been plotted in Fig. 15 in the form of a Strouhal number (Dimensionless frequency, (fD/U_{gs}) against the Lockhart-Martinelli parameter, a type of plot that has been found to correlate frequency data reasonably. The frequency upstream the bend corresponds to the structure frequency measured at the second conductance probe while that of the downstream is the one corresponding to the last conductance probe downstream the bend.

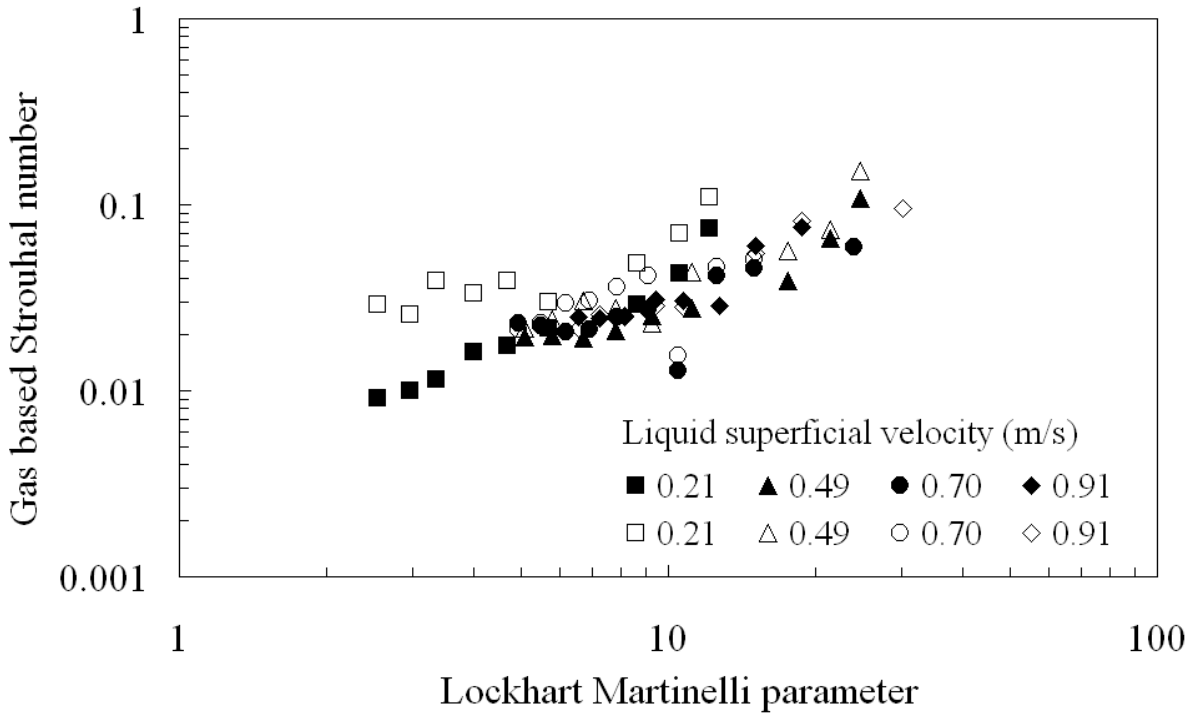

Fig. 15 Gas based Strouhal number against Lockhart-Martinelli parameter upstream and downstream the bend for different liquid superficial velocities, full symbols upstream bend, empty symbols downstream bend

In order to relate the frequency of the periodic structures obtained in the present work to published data, they have been plotted in the form of a Strouhal number against the Lockhart-Martinelli parameter with other data from literature. Figure 16 shows the present data with those of Sànchez Silva et al. [8] obtained in horizontally 90° bend. It can be seen from this figure that both data present the same trend. However the present data lies above the Sanchez Silva et al. line.

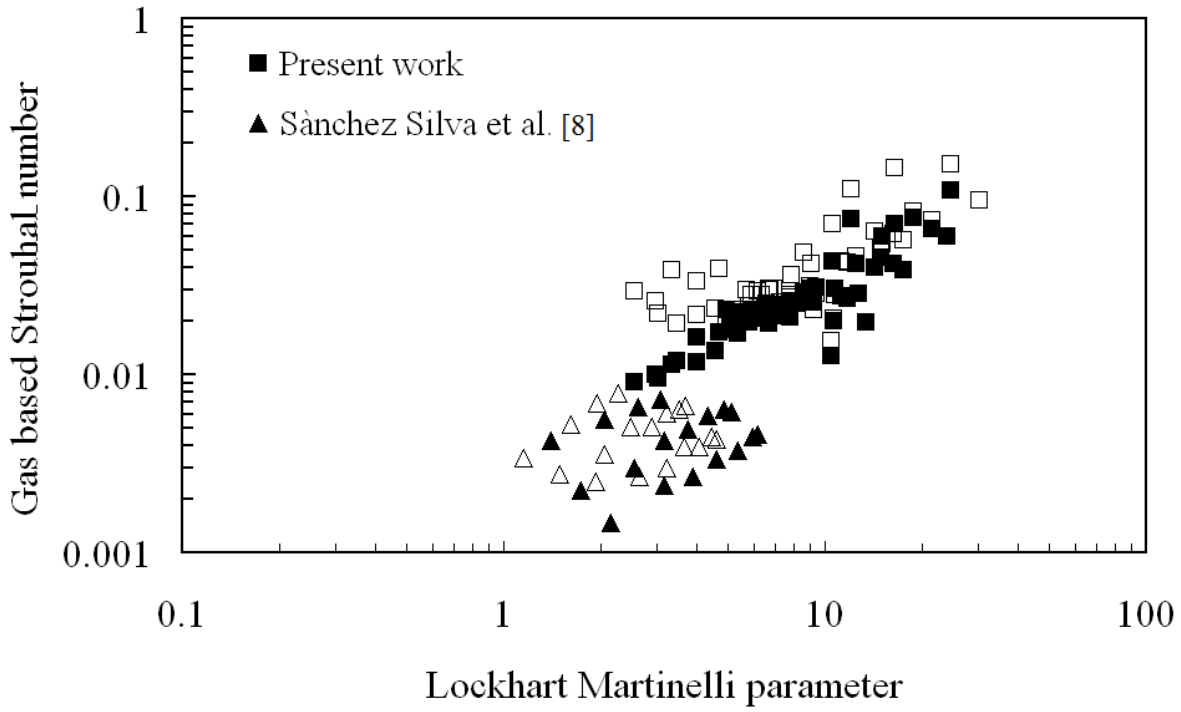

Fig. 16 Gas based Strouhal number against Lockhart-Martinelli parameter upstream and downstream the bend for the whole experiments and Sànchez Silva et al. [8] data obtained with a horizontally 90°.

3.6 Slug length for slug flow

As known the PDF signature of a slug flow is characterized by two peaks. The one at lower void fraction, ε_{GS}, corresponds to the liquid slug. The higher value peak at ε_{GTB} relates to the Taylor bubble or gas plug. These void fractions of liquid slugs and gas plugs can be used to extract quantitative information about the lengths of the liquid slugs and gas plugs or Taylor bubbles when the pipe is positioned vertically. For a vertical pipe an analysis for this was proposed by Khatib and Richardson [22], who implicitly assumed that the length of the liquid slugs and Taylor bubbles were constant. Their approach results in an equation which can be rearranged to give the fractional liquid slug length explicitly as:

$$F = \frac{L_S}{L_u} = \frac{\varepsilon_{GTB} - \varepsilon_G}{\varepsilon_{GTB} - \varepsilon_{GS}} \qquad (2)$$

The length of the slug unit, L_u, the sum of the lengths of Taylor bubbles and of liquid slugs, = L_s + L_{TB}, can be obtained from the velocities, U_S, and frequencies, f, of Taylor bubbles, as L_u =

U_s/f . This can be combined with equation (2) to give the lengths of the two sub-regions. This analysis has been applied to the present data. Measurements of the liquid slugs upstream and downstream the bend using the approach of Khatib and Richardson are plotted in Figs. 17 and 18. From these figures it appears that the slug length vary between 5 and 30 pipe diameter which is close to those reported in the literature for the case of slug flow. Additionally one can remark by comparing the plots of these two figures that slug length increase downstream the bend, the same finding has been reported and can be see in Figs. 19 and 20 despite that for the study of Sànchaz Silva et al. the bend was positioned vertically, showing thus that the increase of the slug length is due principally to the bend and not only to the probably additional effect of gravity.

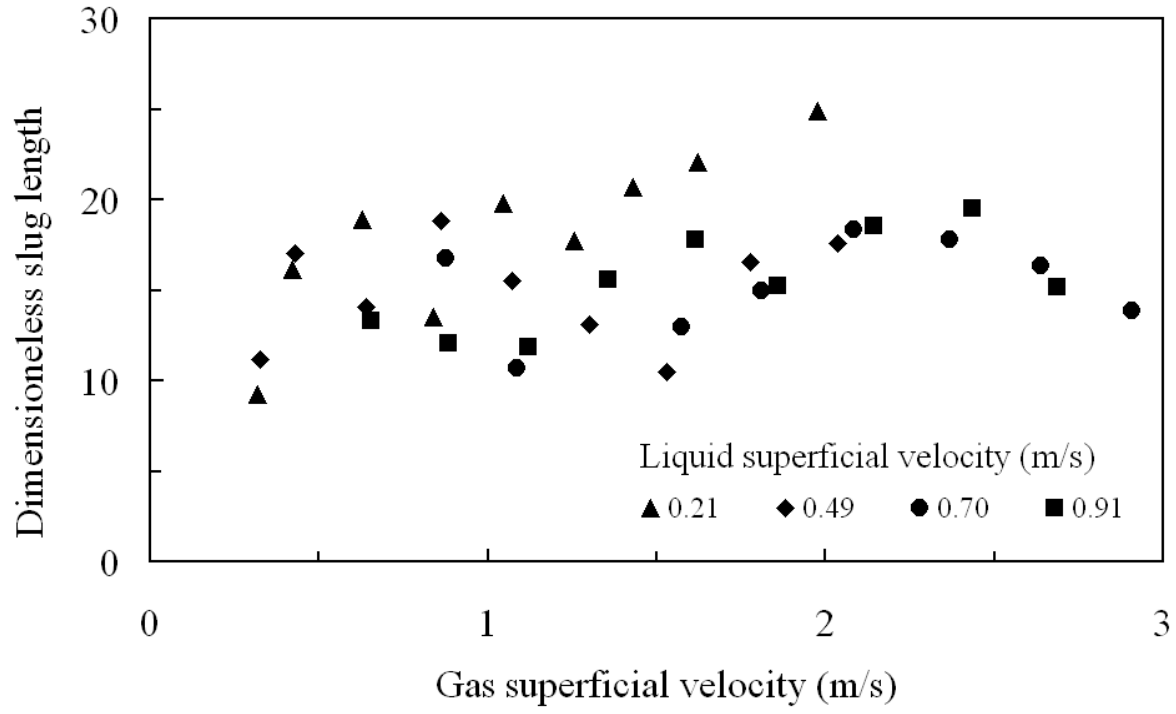

Fig. 17 Liquid slug lengths upstream of the bend

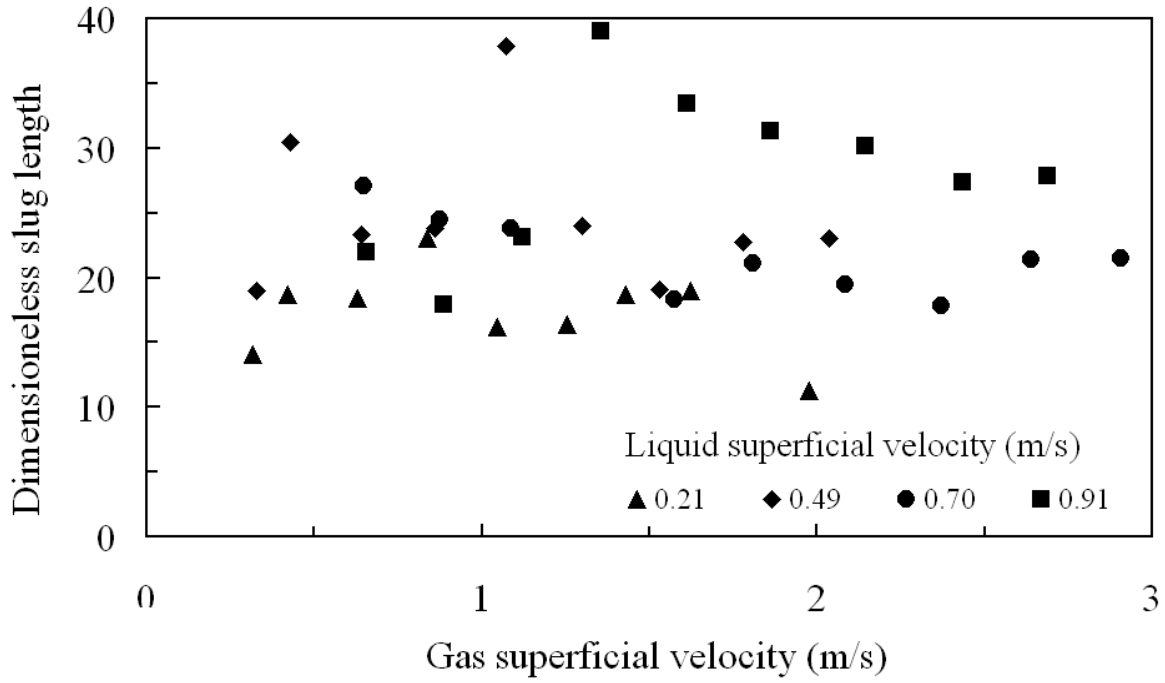

Fig. 18 Liquid slug lengths downstream the bend

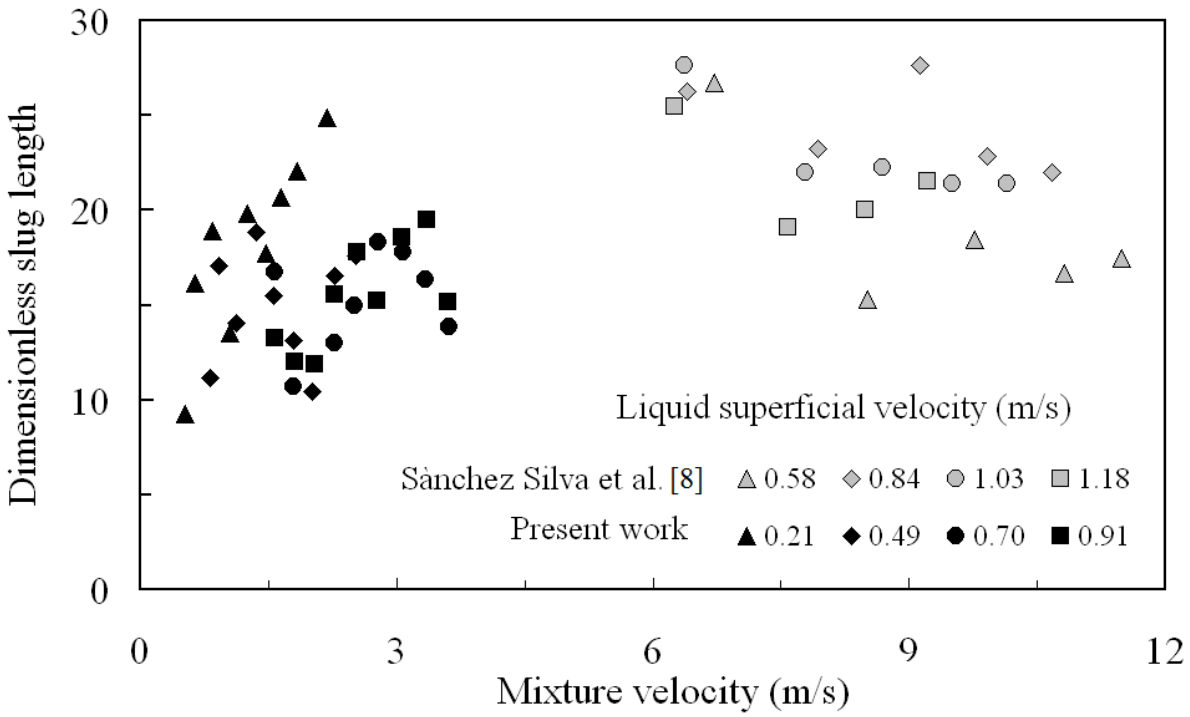

Fig. 19 Liquid slug lengths upstream the bend with the Sànchez Silva et al. [8] data

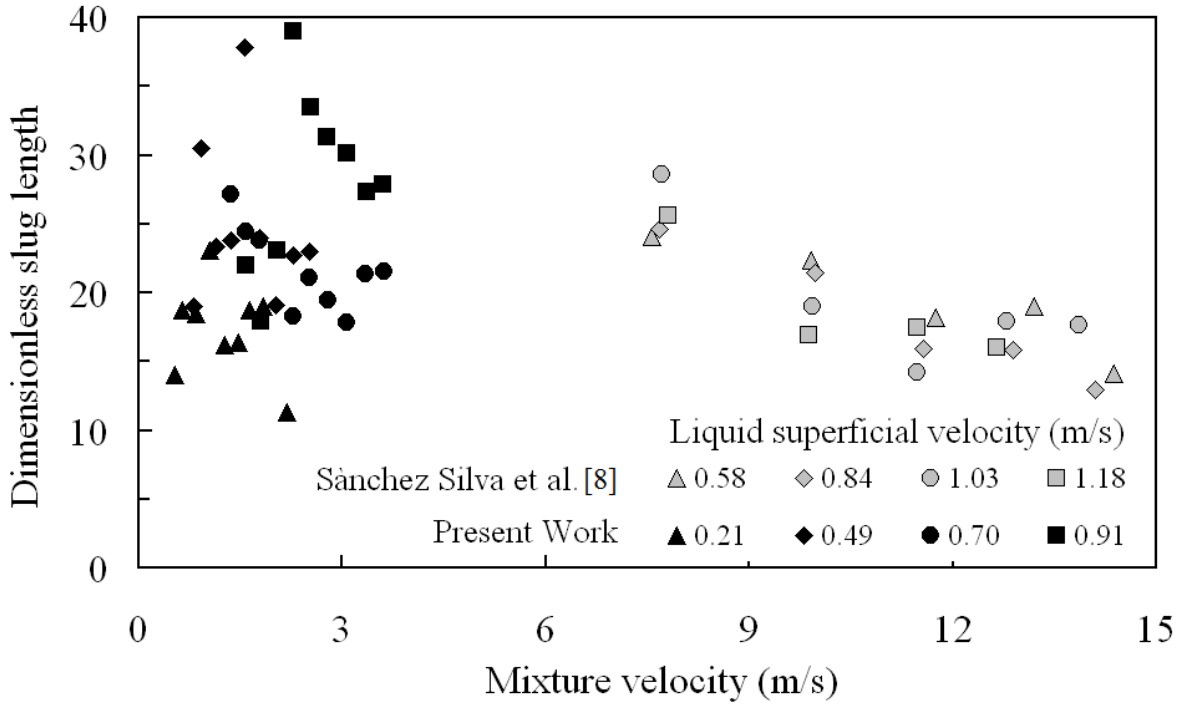

Fig. 20 Liquid slug lengths downstream the bend with the Sànchez Silva et al. [8] data

4. Conclusions

From the present work one can conclude that from the flow conditions:

- Plug, slug and stratified wavy flow occur in the horizontal pipe upstream the bend and slug and churn flow take place in the vertical pipe downstream the bend;
- The void fraction increases with the gas superficial velocity and is higher in the downstream pipe than the upstream pipe.
- The Nicklin et al. correlations predict well the structure velocity for the slug flow pattern in horizontal and in the vertical pipes.
- Some experiments showed persistence of frequency while others showed an increasing in the structure frequency as the flow moved from horizontal to vertical pipe.
- The slug length increase by passing through the bend.

References

[1] A. Azzi, L. Friedel and S. Belaadi, Two-phase gas/liquid flow pressure loss in bends, ForschungimIngenieurwesen. 65 (2000) 309-318.

[2] B.J. Azzopardi, Gas-liquid flows, Begell House, Connecticut (2006).

[3] G.C. Gardner, P.H. Neller, Phase distribution in flow of an air-water mixture round bends and past obstructions at the wall of 76 mm bore tube, Proceedings of the Institution of Mechanical Engineers 184, (1969) p36.

[4] C. Maddock, P.M.C. Lacey, M.A. Patrick, The structure of two-phase flow in a curved pipe, Symposium on Multiphase flow systems, University of Strathclyde, Glasgow, paper J2, published as Institution of Chemical Engineers Symposium, Series No 38 (1974).

[5] M. Abdulkadir, D. Zhao, S. Sharaf, L. Abdulkareem, I.S. Lowndes and B.J. Azzopardi, Interrogating the effect of 90° bends on air-silicone oil flows using advanced instrumentation, Chem. Eng. Sci., 66 (2011) 2453-2467.

[6] A.M. Ribeiro, T.R. Bott, D.M. Jepson, The influence of a bend on drop sizes in horizontal annular two-phase flow. Int. J. Multiphase Flow 27 (2001) 721-728.

[7] K. Sekoguchi, Y. Sato and A. Karayasaki, The influence of mixers, bends and exit section on horizontal two-phase flow, Co Current gas-liquid flow, Plenum Press, (1969).

[8] F. Sánchez Silva, A. Henández Gómez and M. Toledo Velázquez, Experimental characterization of air-water slug flow through a 90° horizontal elbow, Proc. Two-Phase Flow Modeling and Experimentation, G.P. Celata, P.Di Marco and R.K. Shah (Editors) Edizioni ETS, Pisa, (1999).

[9] H.J.W.M. Legius, Propagation of pulsations and waves in two-phase pipe systems, Ph.D. thesis, TechnischeUniversiteit Delft, Delft, Netherlands, (1997).

[10] N.K. Omebere-Iyari and B.J. Azzopardi, Gas/liquid flow in a large riser: effect of upstream configurations, Proc 13th International Conference on Multiphase Production Technology '07 Edinburgh, UK: 13-15 june (2007).

[11] N.A. Tsochatzidis, T.D. Karapantsios, M.V. Vostoglou, A.J. Karabelas, A conductance probe for measuring liquid fraction in pipes and packed beds, Int. J.of Multiphase Flow 18(1992), 653–667.

[12] M. Fossa, 1998. Design and performance of a conductance probe for measuring

liquid fraction in two-phase gas-liquid flow, Flow Meas. Inst., 9 (1998) 103–109.

[13] M. Abdulkadir, D. Zhao, A. Azzi, I.S. Lowndes, B.J. Azzopardi, Two-phase air-water flow through a large diameter vertical 180° bend, Chem. Eng. Sci., 79(2012), 138-152.

[14] T. Morsi T, Contribution au développement d'une chaîne de mesure de conductance dédiée à l'identification des configurations d'écoulements diphasiques. M.Sc. thesis, USTHB University, Algiers, (2012).

[15] T. Morsi T., N. Ababou, A. Ababou, F. Saïdj, S. Arezki S., A. Azzi, Improved electronic conditioning circuit for conductance probe technique. Conférence Internationale sur l'Automatique et la Mécatronique, CIAM'2011, Oran, Algeria. 22-24 November (2011).

[16] G. Costigan and P.B. Whalley, Slug flow regime identification from dynamic void fraction measurements in vertical air-water flows, Int. J. Multiphase Flow, 23(1997) 263–282.

[17] O. C. Jones and N. Zuber, The interrelation between void fraction fluctuations and flow patterns in two-phase flow, Int. J. Multiphase Flow, 2(1975) 273-306.

[18] O. Shoham, Mechanistic modeling of gas-liquid two-phase flow in pipes, Society of Petroleum Engineering, USA, (2005).

[19] H.J.W.M. Legius and H.E.A. van den Akker, Numerical and experimental analysis of transitional gas-liquid pipe flow through a vertical bend. BHRA Group (1997).

[20] D.J. Nicklin, J.O. Wilkes and J.F. Davidson, Two-phase flow in vertical tubes, Trans. Inst. Chem. Eng. 40(1962) 61-68.

[21] L.A. Abdulkareem, Tomographic investigation of gas-oil flow in inclined risers, PhD. Thesis University of Nottingham, (2011).

[22] Z. Khatib and J.F. Richardson, Vertical co-current flow of air and shear thinning suspensions of Kaolin. Chem. Eng. Res. Des. 62(1984) 139-154.

Figure captions

Fig. 1 Schematic diagram of the experimental facility

Fig. 2 Repartition of the conductance probes along the test section

Fig.3 Schematic diagram of the electrical conditioning circuit Morsi et al. [15]

Fig. 4 Flow pattern map in the flow line upstream the 90°bend

Fig. 5 Flow pattern map in the riser downstream of the 90° bend

Fig. 6 Average void fraction time series along the test section upstream and downstream the 90° bend, U_{LS}= 0.91, U_{GS}=1.61 m/s

Fig. 7 PDFs of the void fraction function of the gas superficial velocity (a) upstream the bend (b) downstream the bend; continue curve at the first probe downstream the bend, dashed curve last probe downstream the bend; (liquid superficial velocity of 0.49 m/s).

Fig. 8 Average void fractions versus gas superficial velocity (a) upstream and (b) downstream the bend

Fig. 9 Structural velocities against mixture velocity upstream and downstream the bend

Fig. 10 Evolution of the frequency along the test section for low liquid superficial velocity (= 0.21 m/s)

Fig. 11 Evolution of the frequency along the test section for high liquid superficial velocity (Uls=0.91 m/s)

Fig. 12 Plots of the gas and liquid superficial velocities on the Shoham flow map for the horizontal pipe showing the frequency persistence character. Empty symbol correspond to increase in frequency, filled symbols correspond to persistence of frequency

Fig. 13 Plots of the gas and liquid superficial velocities on the Shoham flow map for the vertical pipe showing the frequency persistence character. Empty symbol correspond to increase in frequency, filled symbols correspond to persistence of frequency

Fig. 14 Effect of inclination on frequency of slugs. Images are time sequences of void distribution across a diameter from Wire Mesh Sensor (WMS) at liquid and gas superficial velocities 0.05 and 0.62 m/s respectively. Abdulkareem [21]

Fig. 15 Gas based Strouhal number against Lockhart-Martinelli parameter upstream and downstream the bend for different liquid superficial velocities, full symbols upstream bend, empty symbols downstream bend

Fig. 16 Gas based Strouhal number against Lockhart-Martinelli parameter upstream and downstream the bend for the whole experiments and Sànchez Silva et al. [7] data obtained with a horizontally 90°.

Fig. 17 Liquid slug lengths upstream of the bend

Fig. 18 Liquid slug lengths downstream the bend

Fig. 19 Liquid slug lengths upstream the bend with the Sànchez Silva et al. [7] data

Fig. 20 Liquid slug lengths downstream the bend with the Sànchez Silva et al. [7] data